SeNic: An Open Source Dataset for sEMG-Based Gesture Recognition in Non-Ideal Conditions

Bo Zhu, Daohui Zhang, Yaqi Chu, Yalun Gu, and Xingang Zhao, *Member, IEEE*

***Abstract*— In order to reduce the gap between the laboratory environment and actual use in daily life of human-machine interaction based on surface electromyogram (sEMG) intent recognition, this paper presents a benchmark dataset of sEMG in non-ideal conditions (*SeNic*). The dataset mainly consists of 8-channel sEMG signals, and electrode shifts from an 3D-printed annular ruler. A total of 36 subjects participate in our data acquisition experiments of 7 gestures in non-ideal conditions, where non-ideal factors of 1) electrode shifts, 2) individual difference, 3) muscle fatigue, 4) inter-day difference, and 5) arm postures are elaborately involved. Signals of sEMG are validated first in temporal and frequency domains. Results of recognizing gestures in ideal conditions indicate the high quality of the dataset. Adverse impacts in non-ideal conditions are further revealed in the amplitudes of these data and recognition accuracies. To be concluded, *SeNic* is a benchmark dataset that introduces several non-ideal factors which often degrade the robustness of sEMG-based systems. It could be used as a freely available dataset and a common platform for researchers in the sEMG-based recognition community. The benchmark dataset *SeNic* are available online via the website (https://github.com/bozhubo/SeNic and https://gitee.com/bozhubo/SeNic).**

***Index Terms*— Surface electromyogram (sEMG), benchmark dataset, gesture recognition, non-ideal conditions.**

I. Introduction

SUBSTANTIAL progress of intelligent rehabilitation equipments such as prostheses and exoskeleton have been made both on mechatronic design and manipulation control [1]. Signals of surface electromyogram (sEMG) are non-invasively acquired from the surface of the skin, and they reflect abundant information related to the limbs motion. Thus, sEMG-based human-robot interaction (HRI) is becoming a mainstream manner to control these rehabilitation equipments [2]. Applications of sEMG-based recognition have produced great importance on the life quality of the disabled. Since the 1960s, sEMG has been used as the on-off control signals of artificial limbs [3]. Gradually, with the development of sensors and microprocessors, high precision sEMG signals are acquired and processed with advanced algorithms. At present, more than 50 discrete gestures are accurately classified and continuous angles of limbs are predicted [4]–[6]. For these purposes, pattern recognition (PR) based methods are always employed, including feature extractions and recognition models [7], [8].

However, PR-based methods always assume that similar distributions are shared between the offline training data and testing data. In real applications, there is existing a vast gap of sEMG-based recognition between accuracies in the ***ideal*** laboratory and those in ***non-ideal*** daily life environments [9]–[12].

In this paper, the environments that involve many adverse impacts of disturbances are called the **non-ideal conditions**, which potentially include 1) electrode shifts, 2) individual difference, 3) muscle fatigue, 4) inter-day difference, 5) arm postures.

1) **Electrode shifts**. An inevitable problem in daily use of prosthetic limbs, is electrode shifts from the doffing and donning of the prosthetic sockets [11], [13]. Displacements away from their default positions and corresponding sEMG changes will reduce the performance of the system.
2) **Individual difference**. Signals of sEMG vary substantially from one person to another. They are changed with the body mass, surface muscular tissue, the way they perform the same gesture, and so on. It is well known that sEMG-based recognition accuracies of inter-subject are far worse than those of intra-subject [14]–[16].
3) **Inter-day difference**. It refers to the variability of using the same sEMG-based prostheses in different days. The inter-day difference often covers two kinds of disturbances. One is the user's adaptation or motor learning to get used to the sEMG-based control system. Especially for the disabled, their muscles are getting rehabilitated

Manuscript received December 7, 2021; revised April 9, 2022; accepted April 21, 2022. Date of publication May 9, 2022; date of current version May 17, 2022. This work was supported in part by the National Natural Science Foundation of China under Grant U20A20197, Grant U1813214, Grant 61903360, and Grant 92048302; in part by the Liaoning Revitalization Talents Program under Grant XLYC1908030; and in part by the China Postdoctoral Science Foundation Funded Project under Grant 2019M661155. *(Corresponding author: Xingang Zhao.)*

This work involved human subjects or animals in its research. Approval of all ethical and experimental procedures and protocols was granted by the Ethical Committee of the Shenyang Institute of Automation.

Bo Zhu and Yalun Gu are with the State Key Laboratory of Robotics, Shenyang Institute of Automation, Chinese Academy of Sciences, Shenyang 110016, China, also with the Institutes for Robotics and Intelligent Manufacturing, Chinese Academy of Sciences, Shenyang 110169, China, and also with the University of Chinese Academy of Sciences, Beijing 100049, China.

Daohui Zhang, Yaqi Chu, and Xingang Zhao are with the State Key Laboratory of Robotics, Shenyang Institute of Automation, Chinese Academy of Sciences, Shenyang 110016, China, and also with the Institutes for Robotics and Intelligent Manufacturing, Chinese Academy of Sciences, Shenyang 110169, China (e-mail: zhaoxingang@sia.cn).

Digital Object Identifier 10.1109/TNSRE.2022.3173708

with rehabilitation training [17]. The other one combines other different causes, such as electrode/socket displacements/shifts from doffing and donning among different days.

4) **Muscle Fatigue**. Muscle fatigue is a physiological phenomenon when muscles are contracted for a long time or repeatedly. Both amplitude and power spectrum density of sEMG are affected by muscle fatigue [18], [19].
5) **Arm postures**. Different postures result from different muscles coordination. These differences ultimately affect sEMG signals and sEMG-based recognition accuracies [20]–[22].

Various non-ideal factors including above-mentioned restrict the developing of sEMG-based systems from laboratory to scenario of actual use. From the experience of rapid development in the field of machine learning, especially in the field of image recognition in recent years, the establishment of data sets is extremely important to promote the development of a pattern recognition related field. As a pointview of Atzori *et al.*, they believed that "*solid benchmarking protocols and publicly available databases*" would promote comparisons among different methods [4]. In deep learning community, the huge dataset ImageNet proposed by Li. Fei. Fei *et al.* has proven to be a milestone [23], [24]. Based on the ImageNet and the competition, impressive progresses are achieved, such as AlexNet [25], ResNet [26], and so on. Thus, it is one of our initial motivations to build a benchmark dataset for sEMG-based pattern recognition to promote the development of EMG-related fields. It is a consensus that "*an open and large dataset is one of the most important contributors in this field*" [23].

Starting from 2012, Atzori *et al.* initiated a project and built a database called *Ninapro* (Non-Invasive Adaptive Hand Prosthetics) [27]–[29]. The database consists of several sub-datasets, covering many currently available acquisitions systems [30]. Many subjects, including the healthy and the disabled, participate in their acquisition experiments. Up to 53 common hand movements in daily life are considered. And baselines of both traditioinal machine learning and deep learning methods are established [4], [31]. It is absolutely an useful promoter for sEMG-based recognition in the field.

Geng *et al.* proposed a deep learning methods with their instantaneous 128-channel high-density EMG signals, and the dataset CapgMyo is hosted in his homepage [32]. Christoph *et al.* also built a 192-channel high-density EMG dataset, CSL-HDEMG [33]. Movements in this dataset are related to fine fingers. But, only five subjects participate in the data acquisition experiments. Also, many pieces of sEMG signals could be freely available from the UCI Machine Learning Repository.

However, these above datasets are collected from the ideal laboratory environments. Many adverse factors in real daily life are not involved. It is our another motivation to build and release a benchmark dataset for sEMG-based recognition, focusing on the detections and eliminations of interferences in non-ideal conditions.

In this paper, we detail the ***SeNic*** (**S**urface **e**lectromyography in **N**on-**i**deal **c**onditions) benchmark dataset. Totally, there are 36 intact-abled sujects in our experiments.

Many subjects participate to the acquisition experiments more than once in different days. The dataset contains two important types of data, one is 8-channel non-invasive sEMG signals, and the other is the electrodes shifted angles represented by a 3D-printed annular ruler. In summary, a total of 24486 trials of experimental data are collected and each trial contains 6-9 seconds of data. Importantly, impacts of the forementioned five factors and their combinations are elabrately involved. The *SeNic* dataset we build provides a platform for researchers to compare their methods and to eliminate adverse impacts in real non-ideal conditions.

The *SeNic* dataset has the following distinct features and contributions.

1) **Rich data.** A large number of subjects participate in the acquisition with tens of thousands of trials.
2) **Non-ideal factors.** As many factors as possible in non-ideal conditions are taken into consideration.
3) **A benchmark dataset.** It can be used to evaluate different sEMG-based recognition methods without collecting different data.
4) **A consumer-grade Myo armband.** Only a consumer-grade sEMG acquisition system is required. It would be easy for reseachers to evalute advanced algorithms in real applications.
5) **Strong validations.** The dataset is comprehensively discussed in this paper, and further validated in our recent studies [13].

The rest of this paper is organized as follows. Section II provides the data acquisition setups and how these factors in non-ideal conditions are involved into the acquisition. Section III explains acquired data and other related files and materials. Section IV describes the basic analyses on the dataset and validates how the gesture recognition is affected by non-ideal impacts. In the last Section V, it makes conclusions and discussions of the dataset, and it looks ahead into what researchers could do by utilizing the benchmark dataset.

II. Methods of Data Acquisition

In this section, data acquisition systems, steps and subjects are detailed. Factors in non-ideal conditions, including electrode shifts, individual difference, muscle fatigue, inter-day difference, and arm postures, are taken into consideration to construct the benchmark dataset.

A. Subjects

This study is reviewed and approved by the Ethical Committee of the Shenyang Institute of Automation. Totally, 36 intact-abled subjects (24.6±2.2 years old, 62.8±12.0 Kg, 170±8.1 cm, 11 females) participate in the following sEMG data acquisition experiments. In order to simulate real usage scenarios as much as possible, all subjects are novices for sEMG data collection. Before the data acquisition, subjects are informed of the detailed experimental motivations, acquisition

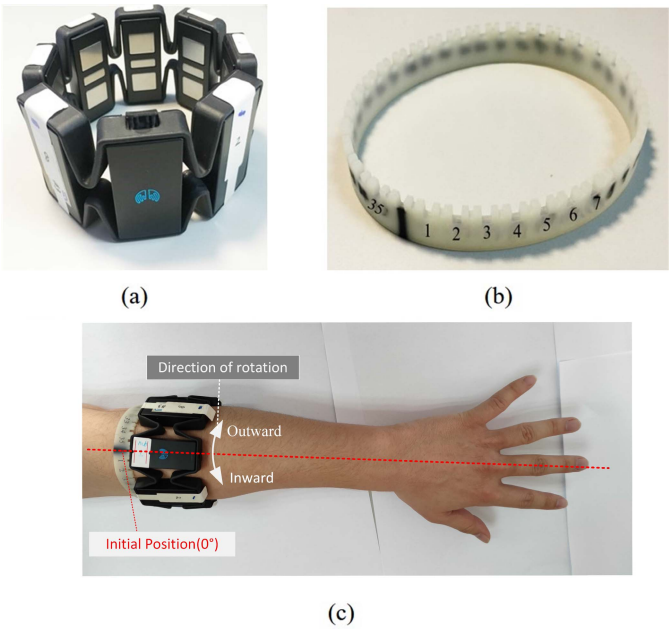

Fig. 1. (a) The Myo armband. (b) The 3D printed annular elastic ruler, where scale numbers are evently marked around the $[0°, 360°]$. (c) The Myo armband and the ruler are worn around the forearm.

steps and potential risks. And they are asked to give the informed consent forms before acquisition experiments.

B. Acquisition Systems

The acquisition setup consists of two import measurement tools: a Myo armband (Thalmic Lab, Canada) for sEMG signals acquisition and an annular elastic ruler for angular measurements, as shown in Fig. 1.

Signals of sEMG with different gestures are acquired by a Myo armband, which is worn around the forearm of subjects. The Myo armband is well known in the sEMG-based recognition field and is applied to many human-computer-interface (HMI) applications. It is a low-cost consumer-grade device having eight differential sEMG channels with a maximum sampling rate of 200Hz to ensure real-time online usage. Acquired data are transmitted to the host computer by the wireless Bluetooth technology.

The other measurement tool is an annular ruler. It is an soft elastic band with the 3D printing technology. Around the band, it is evently divided into 36 parts with 36 big slots, which are marked with numbers from 0 to 35. These slots and marked numbers offer an easy way to locate every electrode around the ruler of $[0°, 360°]$. In the middle of two adjacent big slots, there is a small slot, and thus the minimum precision scale and the estimated accuracy are 5° and 1° respectively. In this way, the ruler is used to keep electrodes fixed during the same acquisition. And for electrode-shifted experiments, shifts relative to the initial positions can be quantified and recorded.

C. Experimental Design

The main steps as shown in Fig. 2 for the data acquisition experiments consist of: a) gesture guide: instruct the participant what action should be done after rest or now; b) data preview for initial validation; c) data storage. Before the data acquisition, subjects are requested to clean the forearm with the alcohol to guarantee a good contact. After familiar with details of the experimental design, they are asked to sit in front of a desk and make one of the seven gestures by following commands shown in the screen.

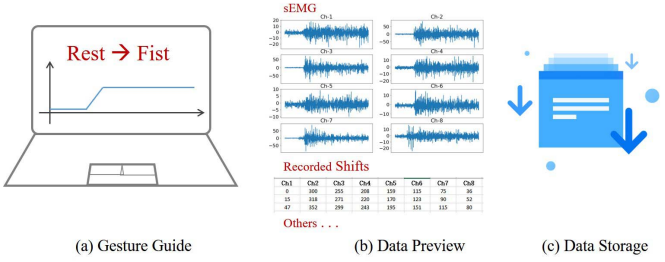

Fig. 2. Main steps for data acquisition: (a) gesture guide, (b) data preview, and (c) data storage.

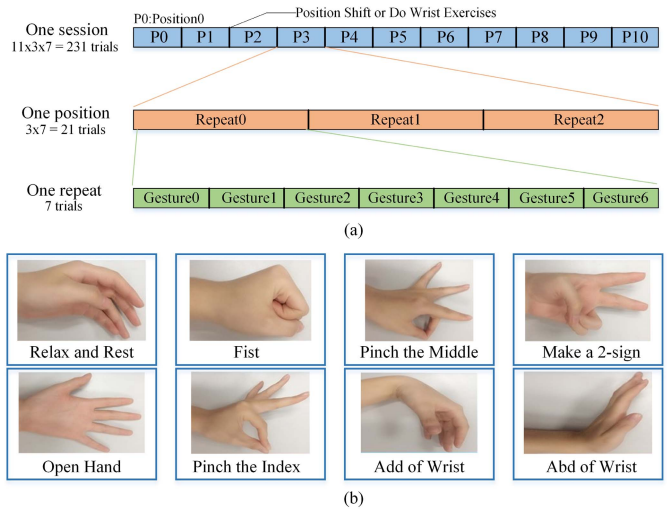

Fig. 3. (a) Schematic diagram of the data collection process for one session. (b) Eight common gestures that subjects would follow for the benchmark dataset.

As shown in Fig. 3 (a), for one session, there are 11 shifted positions. At each position, subjects performed 21 gestures consisting of 7 gestures repeated 3 times. A set of 7 different gestures constituted a repetition, and each gesture corresponds to the EMG signal of one trial. For each trial, the locations of each channel relative to the annular ruler are recorded and saved in Excel files. According to the official requirements of Myo when using its application, users need to align the channel where the Myo's logo is located with the middle finger when the palm is facing the ground. As shown in Fig. 1(c), this position is the initial position of Myo, which is also the 0° position of the annular ruler. In order to maximize the quality of the sEMG signal, the subjects asked to wear Myo on the thickest part of the forearm. At the same time the position of the ruler relative to the elbow will be recorded, which can also prevent a large longitudinal deviation each time it is worn.

The selected gestures are shown in Fig. 3 (b), including {Rest, Fist, Pinch the Middle, Make a 2-sign, Open Hand, Pinch the Index, Add of Wrist, Abd of Wrist}. To make sure the consistency of the gesture labels and their corresponding

data, for each trial, only one gesture is made from the rest state. The start and stop of a new trial are controlled by the subject using the free hand to press the enter key. This can ensure that they are prepared for each trial, which can improve the quality of the data. From the beginning of a trial, subjects make the shown gesture from a 2-second rest state followed by a gesture hold time of 4-7 seconds. That is to say, about 6-9 seconds of data per trial are saved in a comma-separated values(CSV) format file with the name of the gesture.

D. Signal Pre-Processing

No signal pre-processing procedures are conducted. Raw data retrieved from the Myo armband are stored into files. Researchers who plan to validate their algorithms can perform any signal processing.

E. Factors in Non-Ideal Conditions

As one of the most important motivations, factors in non-ideal conditions are taken into consideration, including 1) electrode shifts, 2) individual difference, 3) muscle fatigue, 4) inter-day difference, 5) arm postures. Elaborate acquisition steps upon the experimental design in II-C are conducted to involve these factors. The explainations are as follows:

1) Electrode Shifts: For each subject, Fig. 3(a) shows that eight channels of the Myo armband are shifted in arbitrarily rotary positions around the forearm ranging from 0° to 360° relative to the initial position. Measurements shifts for each channel are quantified and recorded by the annular ruler. In data collection, the direction of rotation, the size of the rotation angle, and the randomness of the rotation of the Myo were taken into consideration. For each subject in each session, 11 different shift positions were collected, among which the first 9 positions were designed, and the last 2 times required the participants to shift randomly. In the first 9 offsets of each acquisition session, 24 subjects were asked to rotate between 30 and 60 degrees in each increment, of which 18 participants rotated inward and 6 subjects rotated outward. The remaining 6 subjects collected data containing small angle offsets, each rotation increment was 10 degrees, and they were rotated in the order of { 0°, 10°, 350°, 20°, 340°, 30°, 330°, 40°, 320°, Random, Random }.

2) Individual Difference: In the benchmark dataset, a total of 36 subjects participated in the data acquisition, which contained a lot of individual differences. All participants' weight, height, forearm length, forearm circumference, and location of the Myo with ruler were recorded.

3) Inter-Day Difference: For many of subjects, their data acquisitions were repeated for several times in different sessions. Specifically, a total of 14 subjects participated in the inter-day data collection, 6 (2 females and 4 males) of them collected 10 times in different 10 sessions and 8 (3 females and 5 males) of them collected 3 times in different 3 days.

4) Muscle Fatigue: To investigate the effect of forearm muscle fatigue on sEMG-based gesture recognition, fatigue-enhanced data were collected from 6 subjects (1 female). When collecting fatigue-enhanced data, the electrodes were no longer offset and instead some wrist exercises were done.

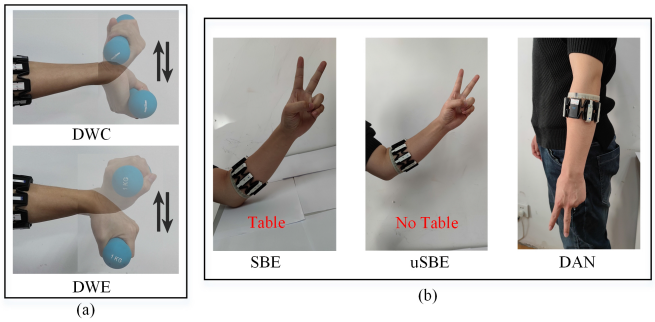

Fig. 4. (a) Exercises for fatigue-enhanced: DWC - Dumbbell Wrist Curl; DWE - Dumbbell Wrist Extension. (b) The Postures: SBE - support the benting elbow on a table; uSBE - unsupport the benting elbow; DAN - drooping arm naturally.

After each collection of 21 gestures (3 sets of repetitions), subjects were required to perform a set of wrist exercises to enhance muscle fatigue. Each set of wrist exercises consists of 5 reps of Dumbbell Wrist Curl (DWC) and 5 reps of Dumbbell Wrist Extension(DWE) with dumbbell load weight of 1Kg as shown in Fig. 4 (a). In total, each participant performed a total of 231 gestures and 100 dumbbell-wrist exercises during a fatigue-enhancing session.

5) Arm Postures: As shown in Fig. 4 (b), in the *SeNic* dataset, three common postures of arm when using Myo were included: support the benting elbow (SBE) on a table, unsupport the benting elbow (uSBE) and drooping arm naturally (DAN). A total of 8 subjects used these three different postures for data collection in three different sessions respectively, and the others used SBE for data collection.

III. Data Records

For each data collection session, a secondary folder contains 231 CSV files from 11 shifted positions with 7 gestures of 3 repetitions. The name of every CSV file is formated as: *emg_pi_rj_gesture.csv*, where $i = 0, 1, \cdots, 10$, $j = 0, 1, 2,$ and the *gesture* stands for one name of the labeled 7 gestures (e.g. *h3\2\emg_p6_r1_fist.csv*). From an example CSV file, *h3\2\emg_p6_r1_fist.csv*, more dataset details are explained as follows:

A. Subjects Information

Who Real names of these subjects were changed to be anonymous as *h0* to *h29*. As mentioned, names can be obtained from the first level folder names. They also appear in the names of the Excel file for recorded electrodes shifts. The basic information of all participants was recorded as shown in Tab. I.

When The number of the names of the second level folders indicates when the subject participates to the acquisition experiment relative to the first time.

B. Shifts in Excel Files

Where Shifted electrode positions relative to the initial position are recorded in some specific Excel files named by *Angle_hx_sessiony.xlsx*, where $hx = 0, 1, \ldots, 29$, and $sessiony = 0, 1, \ldots, 9$.

TABLE I

SUBJECTS' MAIN INFORMATION: GENDER(M: MALE, F: FEMALE), AGE, WEIGHT, HEIGHT, ARM LENGTH (FOREARM LENGTH: THE DISTANCE FROM THE INNER SIDE OF THE ELBOW TO THE WRIST LINE), ARM CIRCUM (THE CIRCUMFERENCE OF THE FOREARM NEXT TO THE RUBBER RING), ER-LENGTH (THE DISTANCE FROM THE INSIDE OF THE ELBOW TO THE RUBBER RING), SESSIONS (NUMBER OF SESSIONS PARTICIPATING IN THE COLLECTION), DESCRIPTION (RI: ROTATE INWARD; RO: ROTATE OUTWARD; RM: SMALL ANGLE ROTATION; FE: FATIGUE ENHANCED)

Name	Gender	Age	Weight/Kg	Height/cm	Arm Length/cm	Arm Circum/cm	ER-Length/cm	Sessions	Description
h0	M	25	78	176	25.2	27.3	5.5	10	RI
h1	F	25	56	167	24.8	24.6	5.2	10	RI
h2	M	26	82	178	25.7	26.8	5.4	10	RI
h3	M	25	72	172	25.3	25.7	5.2	10	RI
h4	M	27	76	174	25.5	26.3	5.2	10	RI
h5	F	22	46	158	22.8	22.4	3.8	10	RI
h6	M	26	74	181	26	26	6.5	3	RI
h7	F	27	54	161	23	21.5	4.8	3	RI
h8	M	24	72	166	23.6	26	4.6	3	RI
h9	M	23	82	188	27.8	26.4	6.8	3	RI
h10	M	23	78	186	27.4	25.9	6.8	3	RI
h11	M	23	58	168	25.3	24	5	3	RI
h12	F	23	43	157	22.2	21.2	3.5	3	RI
h13	F	22	54	163	24.5	24	3.8	3	RI
h14	M	22	56	168	26	27.4	4.7	1	RI
h15	F	22	53	168	24.4	22.5	5.2	1	RI
h16	F	23	47	161	23	21.4	3.4	1	RI
h17	M	31	82	171	25	30	5.8	1	RI
h18	M	25	76	178	24.5	26.4	3.8	1	RO
h19	M	23	63	167	22	25.4	4.4	1	RO
h20	M	23	58	175	26	23	6.5	1	RO
h21	M	22	64	175	25.5	25	5.5	1	RO
h22	M	28	69	186	27	24	6.5	1	RO
h23	F	22	41	157	24.5	20.4	4.2	1	RO
h24	M	23	64	172	24	23	4.6	1	RM
h25	M	25	54	166	23	22	5.8	1	RM
h26	M	24	76	170	24.8	27.3	4.9	1	RM
h27	F	24	47	160	23.8	20.1	4.5	1	RM
h28	F	23	56	161	23	24.5	4.6	1	RM
h29	M	28	63	171	23	23	5.2	1	RM
h30	M	23	54	166	24.9	24.1	4.7	1	FE
h31	M	29	62	172	26.2	25.6	5.3	1	FE
h32	M	27	58	169	25.4	24.3	5.1	1	FE
h33	M	25	72	179	25.8	26	6.5	1	FE
h34	M	28	75	174	25.6	26.8	5.7	1	FE
h35	M	25	46	159	23.8	20.7	4.7	1	FE

C. EMG Data

Surface EMG signals from eight channels are stored in these well-named folders and files. In every CSV file, columns from 1 to 8 represents sEMG signals correspond to 8 channels.

IV. TECHNICAL VALIDATIONS

A. Signal Waveform and Spectrum

Fig. 5 shows raw sEMG signals and their frequency spectrum from eight channels of the Myo armband. In Fig. 5(a), subjects start making shown gestures after about 2-second rest state. The spectrums aound 50 Hz in Fig. 5(b) indicate that the power frequency noise is removed by the Myo hardware or its software algorithms.

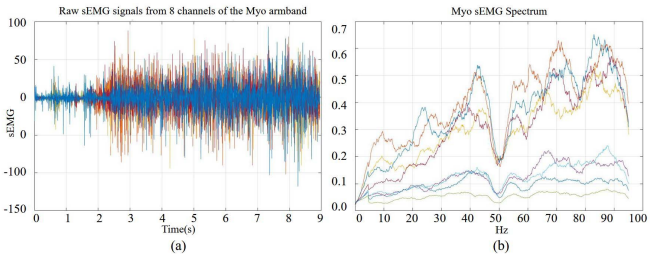

Fig. 5. (a) Raw sEMG signals of one trial from 8 channels. (b) Frequency spectrum of the raw sEMG signals.

B. Gesture Classification in Ideal Conditions

In ideal conditions without impacts of electrode shifts, individual difference, muscle fatigue, inter-day difference and arm postures, validations of the acquired data are conducted first. For each subject, seven gestures are recognized when their corresponding sEMG signals are collected in the same position. We perform the same procedure of feature extraction and classification with the *Ninapro* dataset by Atzori *et al.* [4]. The length of a sample window for calculating features is 250 ms (LW = 50) and the overlap is 200 ms (LI = 10). Five features are considered, including: 1) root mean square (RMS), 2) one common feature in the time domain of the mean absolute value (TD(mav)), 3) the histogram of the raw signals that are divided into 10 bins, 4) the mean absolute value of the continuous wavelet transform by using a Ricker wavelet with 7 levels (CWT(mav)), and 5) the combination of the above four features. Of the same gesture repeated three times at each position, the first two times are used as the

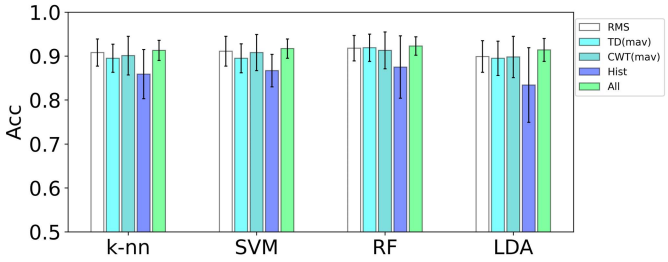

Fig. 6. Gesture recognition results for different classifiers and features in ideal conditions.

training set, and the third time is used as the test set. For the classification, 1) the k-nearest neighbors (k-nn), 2) the Support Vector Machinel (SVM), 3) the random forest (RF), and 4) the Linear Discriminant Analysis (LDA), are conducted and compared as shown in Fig. 6. In ideal conditions, it can be seen from the results that the average accuracy of all classifiers exceeds 90% when using the combined features. General benchmark accuracies are achieved in the proposed dataset.

C. Validations of Non-Ideal Conditions

According the experimental design in II-E, common non-ideal factors are considered in the proposed dataset. In this section, we will detail how these factors affect the sEMG-based recognition.

1) Electrode Shifts: As the acquisition protocol goes, 11 rotary shifted positions are arbitrarily selected to acquire data and corresponding rotary shifts are recorded. As shown in Fig. 7, 11 recorded shifts relative to the initial position are statisticed. These shifts mainly range from 0° to 360°, which indicate arbitrarily rotary positions around the forearm. Among them, the Fig. 7 (a) and Fig. 7 (b) are the large-angle shifts of inward and outward, respectively, and the Fig. 7 (c) shows the situation with small shifts. For all subjects, the last two shifts are random, and the shifts covers the range of 0 to 360 degrees of a circle as shown in Fig. 7.

An obvious feature of the effect of electrode shifts on the sEMG signal is that the sEMG amplitude corresponding to each electrode changes drastically with the change of the shifts. As an example, for the first sesson from *h0* subject in 11 shifted positions, sEMG amplitudes (MAV of eight channels) are displayed, as shown in Fig. 8. It can be seen from the figure that in different positions, these amplitudes are seriously affected by the impact of electrode shifts. These results indicate that the impact of electrode shifts is one of the most important causes to worsen robust sEMG-based recognition.

Furhter to qualify the impact of electrode shifts on gesture recognition, a classifier (SVM with a linear kernel as above) is trained first by the supervised or labeled sEMG data in the initial position. Recognition accuracies in other shifted positions are computed by the pre-trained classifier. The results are recorded in Fig. 9, for small angle shifts, the accuracy decreases as the offset angle increases. For big shifts, these accuracies exhibite a trend that first decline and then rise up, when the shifts range from 0° to 360°. Around the forearm,

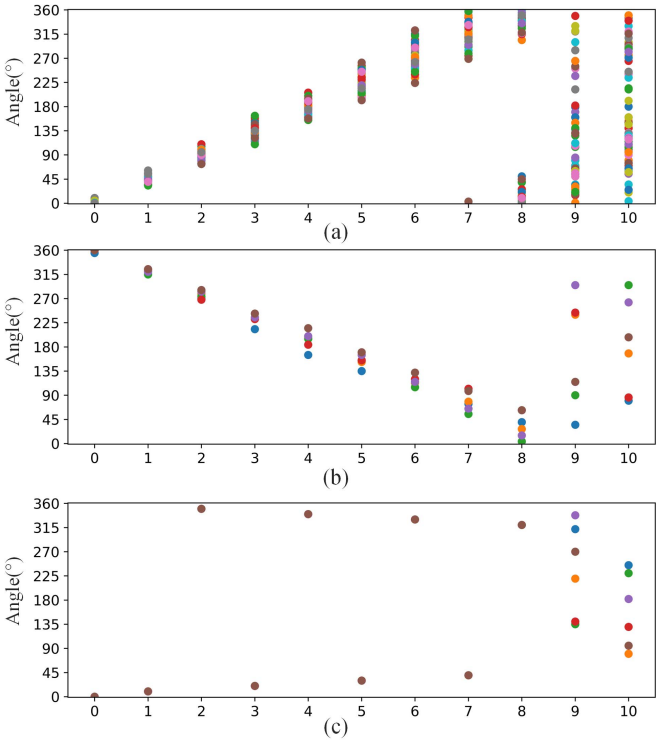

Fig. 7. The angles scatter diagram from all subjects in eleven arbitrary positions (from 0 to 10). (a) Rotation inward. (b) Rotation outward. (c) Rotation with small angle shift in the order of {0°, 10°, 350°, 20°, 340°, 30°, 330°, 40°, 320°, Random, Random }.

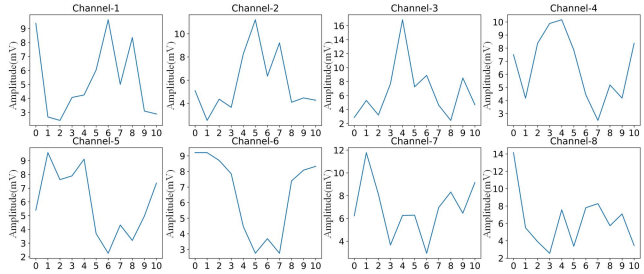

Fig. 8. In these eleven shifted positions from opening a hand gesture, the MAV values of the raw signals from these eight channels.

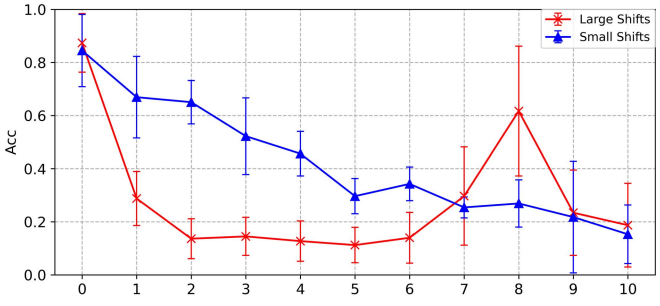

Fig. 9. Recognition results of shifted positions under SVM trained by initial position.

displacements between the current and initial positions go to the maximium when the shift is about 180°.

2) Individual Difference: Different people usually have different muscle sizes and fat thicknesses, and they also have different ways of exerting force. The impact of

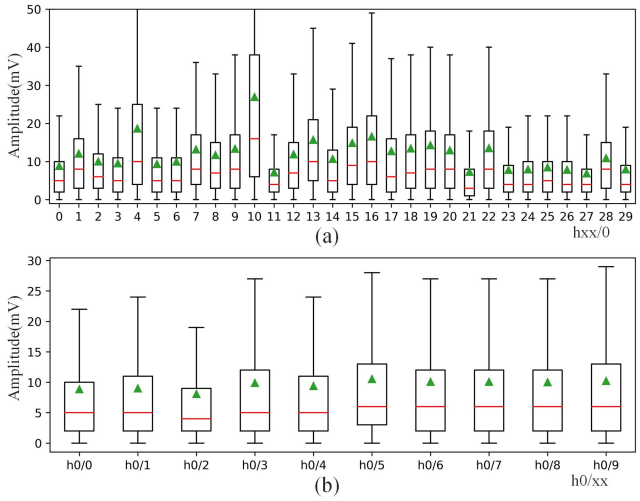

Fig. 10. Effects of individual/inter-day difference on the muscular activity of the Myo armband. The central red bar indicates the median value, the green triangle points represent the mean, and the upper and lower edges are the 25th and 75th percentiles, respectively. The whiskers imply the limitations. (a) Ticks in the x-axis represent different subjects *hxx/0* with first session of each subject. (b) Ticks in the x-axis represent different sessions *h0/xx* from *h0* subject.

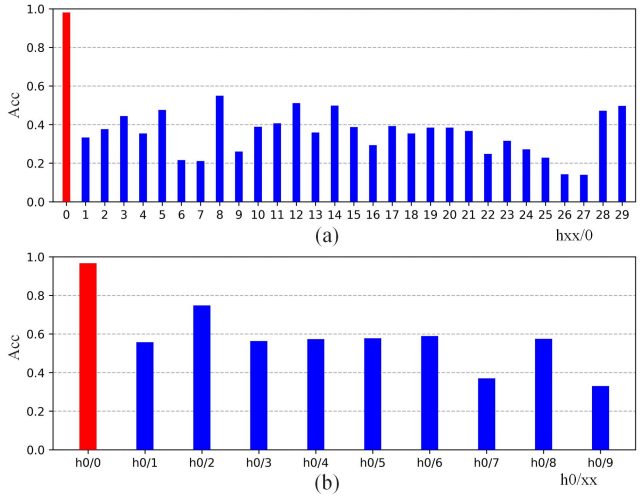

Fig. 11. The influence of individual differences and inter-day differences on recognition results. (a) Accuracies of different subjects of first session under SVM trained by first position from *h0* subject. (b) Accuracies of different sessions under SVM trained by first position from *h0* subject.

individual difference is analysised and compared, as shown in Fig. 10 (a) and Fig. 11 (a). For different subjects (as shown in Fig. 10 (a)), their amplitudes varies widely. They display different distributions around the median values, mean values, or between the 25th and 75th percentiles. Different characteristics of sEMG from different subjects bring a huge challenge for sEMG-based recognition in clinical applications.

For accuracy comparisons (as shown in Fig. 11 (a)), an intial SVM classifier is first trained by the training data of the subject *h0/0*, and tested by the data of other subjects *hxx/0*. It can be seen from the results that, compared with the ideal situation without individual differences, the non-ideal situations with individual differences will cause the recognition results of the ordinary model to become poor.

3) Inter-Day Difference: Compared with individual differences, the impact of inter-day is relatively small for same subject, but there are still effects that cannot be ignored, as shown in Fig. 10 (b) and Fig. 11 (b). When using the first two repetitions of the initial position in the first session of the same subject as the training set to train SVM and use it to recognize gestures at the same position in other sessions, the recognition rate is usually reduced by more than ten percent. Fig. 11 (b) shows the test result of subject *h0*. As the results given in [17], [34], the influence of inter-day will significantly reduce the accuracy of the model. The accuracy of the model decreases with the increase of the interval and this trend has also been verified in our tests.

4) Muscle Fatigue: Muscle fatigue can cause the drift of sEMG features thus it will lead to a decrease in the accuracy of sEMG-based gesture recognition [11], [18], [19], [35]–[38]. The effect of fatigue in *SeNic* is shown in Fig. 12. For the fatigue-enhanced(FE) data, the two repetitions non-fatigued data before exercise were used as the training set to train the model, and the trained model was used for recognition following gradual fatigued data. It can be seen that the recognition accuracy gradually decreases with the increase of acquisition

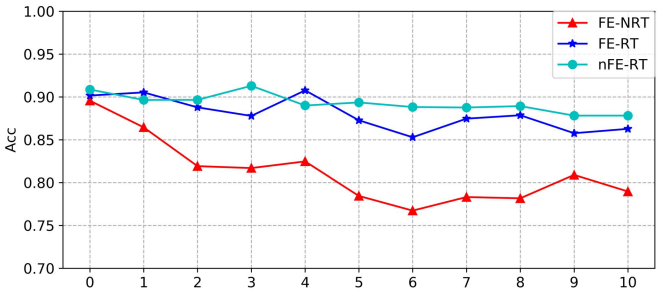

Fig. 12. The influence of fatigue on recognition results. In the figure, The curve represents the average accuracy across subjects. FE means fatigue enhanced data from subjects h30-h35 and nFE means non-fatigue enhanced data from h0-h29. NRT means that the model only uses the first two repetitions of the first position as the training set. RT means that the model is repeatedly trained using the first two repeated data at each position.

time. The accuracy decreases by more than 10% after the 5th position. The recognition accuracy still decreases by 3-5% with increasing fatigue even after retraining the model(RT) using the first two repetitions of each position and using the third repetition as the test set for FE data. Similarly, accuracy dropped by 2-3% for non-fatigue enhancement(nFE).

5) Arm Postures: The impacts of arm postures have been investigated by many researchers [20], [21]. The three different postures shown in Fig. 4 were collected in three different sessions. In order to verify the effect of postures on the recognition results in the *SeNic*, the EMG signals from the first session are used for training the SVM model. The trained SVM is used for the remaining two postures tests. Compared to the ideal situation, the 2 different postures from 8 subjecs caused a 31.95% decrease in average accuracy. This reduction also covers the effect of inter-day difference. As a comparison, the same method is used for the first three sessions of the 6 subjects that collected data while the posture remains same. The test results show that the average accuracy rate is only reduced by 19.33% without the influence of different postures. In other words, different postures will reduce the recognition rate of ordinary models by more than 10%.

D. Limitations of the SeNic

Although the dataset introduces numerous non-ideal conditions to solve some gaps in sEMG technology from the laboratory to daily applications or commercial products, there are still many restrictions on its use. First of all, the maximum sampling rate of the data collection Myo system is 200Hz. According to Shannon's sampling theorem, components exceeding 100Hz cannot be obtained from the dataset. However, the 200Hz sampling rate is sufficient for recognizing several gestures in daily use from the fact that Myo bracelets are widely used in EMG recognition and related data sets in *Ninapro* are widely used [4], [27]–[29]. Secondly, due to the feature that Myo makes a ring, *SeNic* currently mainly introduces rotational shifts, and does not consider the longitudinal offsets. For the EMG differences collected by the forearm, considering that the direction of the muscle fibers is basically parallel to the forearm, the influence of longitudinal offsets is smaller than that of rotational shifts [39], [40]. In addition, it should be noted that the participants in this dataset are all healthy people, and the difference should be noted when transferring the corresponding research methods to the disabled.

V. Discussions and Conclusion

Relying on the consumer-grade Myo armband, this paper presents an sEMG benchmark dataset for studying the robustness of sEMG-based gesture recognition in real applications. Factors involved in these non-ideal conditions include 1) electrode shifts, 2) individual difference, 3) inter-day difference, 4) muscle fatigue, and 5) arm postures. Adverse impacts of these factors are detailed and compared between ideal and non-ideal conditions, especially in the aspect of the gesture recognition accuracy. It is concluded that these factors are main causes to degrade the sEMG-based recognition performance.

It should be noted that in the field of intent recognition based on EMG, there is no consensus on the best acquisition protocol. Pizzolato *et al.* compared different acquisition setups on hand movement classification tasks [30]. The *Ninapro* database they built includes several different sEMG datasets and lays foundation for developing advanced methods to improve sEMG-based performance in **relatively ideal** conditions and comparisons among these methods. The benchmark dataset *SeNic* we built in the non-ideal conditions could be an extended one of the *Ninapro*. On the one hand, more attentions should be paid in impacts of adverse factors in real applications, and datasets in different situations are necessary to be built and shared in the sEMG-base recognition community. On the other hand, the gap between achievements in laboratories and daily lifes could be bridged with the help of *SeNic*. It provides a platform for comparisons between *ideal* and *non-ideal* conditions, especially for comparisons among many potential methods. If researchers can find a model to improve the performance of *SeNic* dataset, it will play a huge role in solving the problem of the gap between sEMG applications from the laboratory to the daily life.

In many real applications, more than one causes have serious impacts on the sEMG-based performance. For example, one subject continuously uses an sEMG-based prosthese for a long time, impacts of electrode shifts, muscle fatigue, and even the perspiration [41] happened at the same time. It is essential that potential methods or frameworks have abilities to tackle all possible factors. There are several different approaches that have the potential to address interference in these non-ideal situations [9], [12]. Most of these methods try to improve the performance of a specific non-ideal factor based on prior knowledge [11], [13]. An experience that can be learned from the field of image recognition and natural language processing is that the community can create a large number of datasets to find some features or models such as CNN, LSTM, transformer etc. that can be a strong baseline for most sEMG-based recognition task through big data driven methods [23]–[26]. In addition, transfer learning also shows potential to improve performance for some non-ideal factors such as individual differences and inter-day differences when the amount of data is not particularly large [42], [43].

According to our previous experience of sEMG and its application research [5], [44]–[48], especially for research under non-ideal conditions [11], [13], [49], designing experimental paradigms and collecting experimental data will consume a lot of time and energy. However, what is more important in the research process is usually the analysis of sEMG features and the improvement of models. The open source of data and methods can increase the efficiency of researchers in related research, reduce the time spent on unnecessary experimental design and data collection, and enable researchers to focus on solving more important problems.

As future work, more improvements of the benchmark dataset will be required from two aspects: 1) more data by other sEMG acquisition systems and from other situations, and 2) potential methods to remove adverse impacts of these factors will be further studied.

Acknowledgment

The authors would like to thank the State Key Laboratory of Robotics for supporting the advanced experimental equipments and excellent environment. They also would thank many members in the Group of Medical Rehabilitation Robotics (Shenyang Institute of Automation) for participating in sEMG signals acquisition experiments. They would like to thank Z. Li and G. Qu for their helps in the *SeNic* dataset establishment and data acquisition.

References

[1] M. A. Price, P. Beckerle, and F. C. Sup, "Design optimization in lower limb prostheses: A review," *IEEE Trans. Neural Syst. Rehabil. Eng.*, vol. 27, no. 8, pp. 1574–1588, Aug. 2019.

[2] D. Farina *et al.*, "The extraction of neural information from the surface EMG for the control of upper-limb prostheses: Emerging avenues and challenges," *IEEE Trans. Neural Syst. Rehabil. Eng.*, vol. 22, no. 4, pp. 797–809, Jul. 2014.

[3] D. S. Childress, F. Hampton, C. Lambert, R. G. Thompson, and M. Schrodt, "Myoelectric immediate postsurgical procedure: A concept for fitting the upper-extremity amputee," *Artif. Limbs*, vol. 13, no. 2, p. 55, 1969.

[4] M. Atzori *et al.*, "Electromyography data for non-invasive naturally-controlled robotic hand prostheses," *Sci. Data*, vol. 1, Dec. 2014, Art. no. 140053.

[5] J. Han, Q. Ding, A. Xiong, and X. Zhao, "A state-space EMG model for the estimation of continuous joint movements," *IEEE Trans. Ind. Electron.*, vol. 62, no. 7, pp. 4267–4275, Jul. 2015.

[6] J. M. Hahne, M. A. Schweisfurth, M. Koppe, and D. Farina, "Simultaneous control of multiple functions of bionic hand prostheses: Performance and robustness in end users," *Sci. Robot.*, vol. 3, no. 19, Jun. 2018, Art. no. eaat3630.

[7] D. Xiong, D. Zhang, X. Zhao, and Y. Zhao, "Deep learning for EMG-based human-machine interaction: A review," *IEEE/CAA J. Automat. Sinica*, vol. 8, no. 3, pp. 512–533, Mar. 2021.

[8] D. Qi-Chuan, X. An-Bin, Z. Xin-Gang, and H. Jian-Da, "A review on researches and applications of sEMG-based motion intent recognition methods," *Acta Automatica Sinica*, vol. 42, no. 1, pp. 13–25, 2016.

[9] H. Xu and A. Xiong, "Advances and disturbances in sEMG-based intentions and movements recognition: A review," *IEEE Sensors J.*, vol. 21, no. 12, pp. 13019–13028, Jun. 2021.

[10] I. Kyranou, S. Vijayakumar, and M. S. Erden, "Causes of performance degradation in non-invasive electromyographic pattern recognition in upper limb prostheses," *Frontiers Neurorobotics*, vol. 12, p. 58, Sep. 2018.

[11] Q. Ding, X. Zhao, J. Han, C. Bu, and C. Wu, "Adaptive hybrid classifier for myoelectric pattern recognition against the interferences of outlier motion, muscle fatigue, and electrode doffing," *IEEE Trans. Neural Syst. Rehabil. Eng.*, vol. 27, no. 5, pp. 1071–1080, May 2019.

[12] T. Bao, S. Q. Xie, P. Yang, P. Zhou, and Z. Zhang, "Towards robust, adaptive and reliable upper-limb motion estimation using machine learning and deep learning—A survey in myoelectric control," *IEEE J. Biomed. Health Informat.*, early access, Mar. 16, 2022, doi: 10.1109/JBHI.2022.3159792.

[13] Z. Li, X. Zhao, G. Liu, B. Zhang, D. Zhang, and J. Han, "Electrode shifts estimation and adaptive correction for improving robustness of sEMG-based recognition," *IEEE J. Biomed. Health Informat.*, vol. 25, no. 4, pp. 1101–1110, Apr. 2021.

[14] C. Castellini, A. E. Fiorilla, and G. Sandini, "Multi-subject/daily-life activity EMG-based control of mechanical hands," *J. Neuroeng. Rehabil.*, vol. 6, no. 1, p. 41, Dec. 2009.

[15] R. N. Khushaba, "Correlation analysis of electromyogram signals for multiuser myoelectric interfaces," *IEEE Trans. Neural Syst. Rehabil. Eng.*, vol. 22, no. 4, pp. 745–755, Jul. 2014.

[16] T. Bao, S. A. R. Zaidi, S. Xie, P. Yang, and Z.-Q. Zhang, "Inter-subject domain adaptation for CNN-based wrist kinematics estimation using sEMG," *IEEE Trans. Neural Syst. Rehabil. Eng.*, vol. 29, pp. 1068–1078, 2021.

[17] M. Ison, I. Vujaklija, B. Whitsell, D. Farina, and P. Artemiadis, "High-density electromyography and motor skill learning for robust long-term control of a 7-DoF robot arm," *IEEE Trans. Neural Syst. Rehabil. Eng.*, vol. 24, no. 4, pp. 424–433, Apr. 2015.

[18] J.-H. Song, J.-W. Jung, S.-W. Lee, and Z. Bien, "Robust EMG pattern recognition to muscular fatigue effect for powered wheelchair control," *J. Intell. Fuzzy Syst.*, vol. 20, no. 1, pp. 3–12, 2009.

[19] L. Li, H. Shin, X. Li, S. Li, and P. Zhou, "Localized electrical impedance myography of the biceps brachii muscle during different levels of isometric contraction and fatigue," *Sensors*, vol. 16, no. 4, p. 581, Apr. 2016.

[20] K.-H. Park, H.-I. Suk, and S.-W. Lee, "Position-independent decoding of movement intention for proportional myoelectric interfaces," *IEEE Trans. Neural Syst. Rehabil. Eng.*, vol. 24, no. 9, pp. 928–939, Sep. 2015.

[21] J. Liu, D. Zhang, X. Sheng, and X. Zhu, "Quantification and solutions of arm movements effect on sEMG pattern recognition," *Biomed. Signal Process. Control*, vol. 13, pp. 189–197, Sep. 2014.

[22] Y. Geng, P. Zhou, and G. Li, "Toward attenuating the impact of arm positions on electromyography pattern-recognition based motion classification in transradial amputees," *J. Neuroeng. Rehabil.*, vol. 9, no. 1, p. 74, 2012.

[23] J. Deng, W. Dong, R. Socher, L.-J. Li, K. Li, and L. Fei-Fei, "ImageNet: A large-scale hierarchical image database," in *Proc. IEEE Conf. Comput. Vis. Pattern Recognit.*, Jun. 2009, pp. 248–255.

[24] O. Russakovsky *et al.*, "ImageNet large scale visual recognition challenge," *Int. J. Comput. Vis.*, vol. 115, no. 3, pp. 211–252, Dec. 2015.

[25] A. Krizhevsky, I. Sutskever, and G. E. Hinton, "Imagenet classification with deep convolutional neural networks," in *Proc. Adv. Neural Inf. Process. Syst.*, 2012, pp. 1097–1105.

[26] K. He, X. Zhang, S. Ren, and J. Sun, "Deep residual learning for image recognition," in *Proc. IEEE Conf. Comput. Vis. Pattern Recognit.*, Jun. 2016, pp. 770–778.

[27] M. Atzori *et al.*, "Building the ninapro database: A resource for the biorobotics community," in *Proc. 4th IEEE RAS EMBS Int. Conf. Biomed. Robot. Biomechatronics (BioRob)*, Jun. 2012, pp. 1258–1265.

[28] M. Atzori *et al.*, "Characterization of a benchmark database for myoelectric movement classification," *IEEE Trans. Neural Syst. Rehabil. Eng.*, vol. 23, no. 1, pp. 73–83, Jan. 2014.

[29] M. Atzori and H. Müller, "The ninapro database: A resource for sEMG naturally controlled robotic hand prosthetics," in *Proc. 37th Annu. Int. Conf. IEEE Eng. Med. Biol. Soc. (EMBC)*, Aug. 2015, pp. 7151–7154.

[30] S. Pizzolato, L. Tagliapietra, M. Cognolato, M. Reggiani, H. Müller, and M. Atzori, "Comparison of six electromyography acquisition setups on hand movement classification tasks," *PLoS ONE*, vol. 12, no. 10, Oct. 2017, Art. no. e0186132.

[31] M. Atzori, M. Cognolato, and H. Müller, "Deep learning with convolutional neural networks applied to electromyography data: A resource for the classification of movements for prosthetic hands," *Frontiers Neurorobot.*, vol. 10, p. 9, Sep. 2016.

[32] W. Geng, Y. Du, W. Jin, W. Wei, Y. Hu, and J. Li, "Gesture recognition by instantaneous surface EMG images," *Sci. Rep.*, vol. 6, p. 36571, Nov. 2016.

[33] C. Amma, T. Krings, J. Böer, and T. Schultz, "Advancing muscle-computer interfaces with high-density electromyography," in *Proc. 33rd Annu. ACM Conf. Hum. Factors Comput. Syst.*, 2015, pp. 929–938.

[34] J. He, D. Zhang, N. Jiang, X. Sheng, D. Farina, and X. Zhu, "User adaptation in long-term, open-loop myoelectric training: Implications for EMG pattern recognition in prosthesis control," *J. Neural Eng.*, vol. 12, no. 4, Jun. 2015, Art. no. 046005.

[35] M. R. Al-Mulla, F. Sepulveda, M. Colley, and A. Kattan, "Classification of localized muscle fatigue with genetic programming on sEMG during isometric contraction," in *Proc. Annu. Int. Conf. IEEE Eng. Med. Biol. Soc.*, Sep. 2009, pp. 2633–2638.

[36] P. K. Artemiadis and K. J. Kyriakopoulos, "An EMG-based robot control scheme robust to time-varying EMG signal features," *IEEE Trans. Inf. Technol. Biomed.*, vol. 14, no. 3, pp. 582–588, May 2010.

[37] E. Kwatny, D. H. Thomas, and H. G. Kwatny, "An application of signal processing techniques to the study of myoelectric signals," *IEEE Trans. Biomed. Eng.*, vol. BME-17, no. 4, pp. 303–313, Oct. 1970.

[38] E. Park and S. G. Meek, "Fatigue compensation of the electromyographic signal for prosthetic control and force estimation," *IEEE Trans. Biomed. Eng.*, vol. 40, no. 10, pp. 1019–1023, Oct. 1993.

[39] S. Muceli, N. Jiang, and D. Farina, "Extracting signals robust to electrode number and shift for online simultaneous and proportional myoelectric control by factorization algorithms," *IEEE Trans. Neural Syst. Rehabil. Eng.*, vol. 22, no. 3, pp. 623–633, May 2013.

[40] A. J. Young, L. J. Hargrove, and T. A. Kuiken, "Improving myoelectric pattern recognition robustness to electrode shift by changing interelectrode distance and electrode configuration," *IEEE Trans. Biomed. Eng.*, vol. 59, no. 3, pp. 645–652, Mar. 2011.

[41] M. Abdoli-Eramaki, C. Damecour, J. Christenson, and J. Stevenson, "The effect of perspiration on the sEMG amplitude and power spectrum," *J. Electromyogr. Kinesiol.*, vol. 22, no. 6, pp. 908–913, Dec. 2012.

[42] U. Cãtãllard *et al.*, "Deep learning for electromyographic hand gesture signal classification using transfer learning," *IEEE Trans. Neural Syst. Rehabil. Eng.*, vol. 27, no. 4, pp. 760–771, Oct. 2019.

[43] C. Prahm *et al.*, "Counteracting electrode shifts in upper-limb prosthesis control via transfer learning," *IEEE Trans. Neural Syst. Rehabil. Eng.*, vol. 27, no. 5, pp. 956–962, May 2019.

[44] D. Xiong, D. Zhang, X. Zhao, Y. Chu, and Y. Zhao, "Synergy-based neural interface for human gait tracking with deep learning," *IEEE Trans. Neural Syst. Rehabil. Eng.*, vol. 29, pp. 2271–2280, 2021.

[45] Q. Ding, J. Han, and X. Zhao, "Continuous estimation of human multi-joint angles from sEMG using a state-space model," *IEEE Trans. Neural Syst. Rehabil. Eng.*, vol. 25, no. 9, pp. 1518–1528, Sep. 2017.

[46] F. Wang, D. Zhang, S. Hu, B. Zhu, F. Han, and X. Zhao, "Brunnstrom stage automatic evaluation for stroke patients by using multi-channel sEMG," in *Proc. 42nd Annu. Int. Conf. IEEE Eng. Med. Biol. Soc. (EMBC)*, Jul. 2020, pp. 3763–3766.

[47] B. Zhu, D. Zhang, Y. Chu, X. Zhao, L. Zhang, and L. Zhao, "Face-computer interface (FCI): Intent recognition based on facial electromyography (fEMG) and online human-computer interface with audiovisual feedback," *Frontiers Neurorobotics*, vol. 15, p. 96, Jul. 2021.

[48] Z. Li *et al.*, "A temporally smoothed MLP regression scheme for continuous knee/ankle angles estimation by using multi-channel sEMG," *IEEE Access*, vol. 8, pp. 47433–47444, 2020.

[49] Q. Ding, J. Han, X. Zhao, and Y. Chen, "Missing-data classification with the extended full-dimensional Gaussian mixture model: Applications to EMG-based motion recognition," *IEEE Trans. Ind. Electron.*, vol. 62, no. 8, pp. 4994–5005, Aug. 2015.